Available online at www.eccomasproceedia.org
Eccomas Proceedia COMPDYN (2021) 5005-5014

ECCOMAS
Proceedia

COMPDYN 2021
8th ECCOMAS Thematic Conference on
Computational Methods in Structural Dynamics and Earthquake Engineering
M. Papadrakakis, M. Fragiadakis (eds.)
Streamed from Athens, Greece, 28 - 30 June 2021

MODELLING THE IMPACT OF GAPPING BEHAVIOUR ON MONOPILE MOUNTED OFFSHORE WIND TURBINE DYNAMICS

Stephen A. Williams[1], **Loizos Pelecanos**[1], **and Antony P. Darby**[1]

[1] Department of Architecture and Civil Engineering
University of Bath
Claverton Down, Bath, BA27AY, UK
e-mail: {sw2007,lp640,absapd}@bath.ac.uk

Abstract. *Increased demand for renewable energy production has stimulated interest in the offshore wind turbine (OWT) industry as a viable solution, and with OWTs growing larger in scale, further research is required into the dynamics of these newer structures. The majority of installed OWTs to date are built upon monopile foundations, and it is widely acknowledged that the current design methods for offshore piles are not appropriate for the large diameter piles required. This paper uses a novel pile-soil gapping algorithm to simulate the effects of degradation to the soil conditions in the sea bed. Using a 1D Winkler beam-spring approach, a dynamic model is validated for prediction of the natural frequencies of several OWT case studies, and the gapping algorithm is shown to reproduce well the reduction in natural frequency likely attributed to soil degradation measured from an OWT in Kentish Flats wind farm. It is found through the simulation of rotor-stop tests that the presence of gapping decreases the measured natural frequency, and this effect is greater for the monopile foundations with a smaller slenderness ratio.*

Keywords: SSI, Gapping, Offshore Wind Turbines, Monopile, Winkler

ISSN:2623-3347
Peer-review under responsibility of the organizing committee of COMPDYN 2021.
doi: 10.7712/120121.8845.18612

1 INTRODUCTION

The use of offshore wind power as a means of renewable electricity generation is becoming ever more popular, and is set to continue to grow as an industry. Offshore wind turbines (OWTs) can be mounted on a variety of foundations, including jacket structures, gravity bases, tripods and more recently floating foundation concepts. However, the most common choice is the monopile, due to its relatively simple and economical production. Monopiles are typically long and slender foundations that flex to accomodate the motion of the supported structure. But as energy demands grow, and the construction technology improves, OWTs are rapidly increasing in size, increasing their energy output, and requiring larger diameter and, therefore, more rigid foundations than previously detailed in design recommendations.

OWTs consist of a monopile foundation, a long flexible tower above the water line, and a substructure connecting the two. The nacelle, containing the generators and blade assembly, is affixed atop the tower. Due to the top-heavy nature of this arrangement, OWTs are dynamically sensitive structures, and as such due care must be taken to avoid unwanted resonances once operational. The OWT design paradigm can be described with three categories; stiff-stiff, soft-stiff, and soft-soft [1], referring to the flexibility of the support structure. Displayed in Figure 1, the OWT experiences four main driving frequencies. Wind and wave loading peaks at low frequencies around 0.1 Hz. The rotation of the rotor within the nacelle exerts an additional force on the system, at a frequency of 1P, ranging from around 0.1 to 0.3 Hz. The 3P loading arises from the blade shadowing force exerted on the OWT from the air deficiency created by the blades sweeping infront of the tower as they rotate, with a frequency of 3*1P for a three-bladed turbine, and 2*1P for a two-bladed turbine (i.e 2P rather than 3P). In response to these driving forces, the soft-soft design regime places the natural frequency of the superstructure less than 1P, the soft-stiff between 1P and 3P and the stiff-stiff above 3P. Since the soft-soft is in danger of becoming excited by environmental loading, and the stiff-stiff requires too much steel to be economically viable, the soft-stiff approach is the most suitable. The bandwidth of non-resonant frequencies is narrow, so it is important to be aware of the the natural frequency of the structure upon installation, and also how it may vary during the operational lifetime.

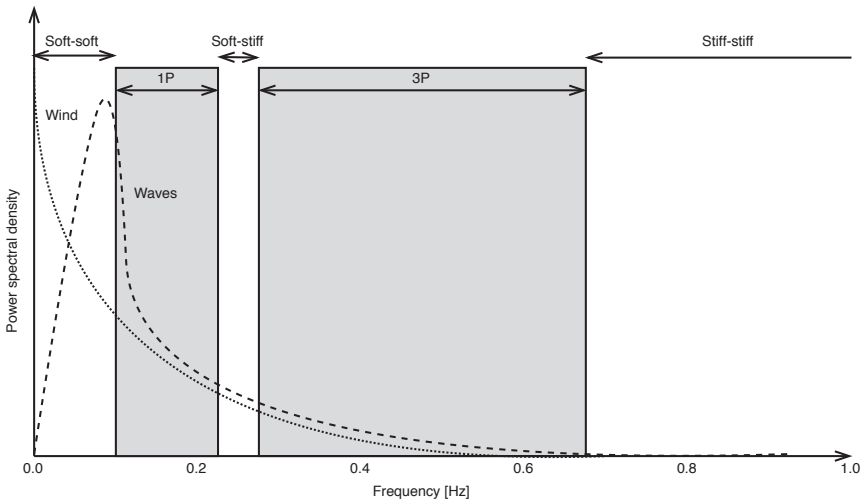

Figure 1: Example power spectrum of an OWT, showing rotor frequency 1P, blade passing frequency 3P, and wind and wave spectra (Figure adapted from [1]).

OWTs experience cyclic loading in the lateral direction from wind and waves, and during its expected operational lifetime of 25-30 years may experience billions of cycles [2]. Currently, the design methods employ beam-on-nonlinear-Winkler-foundation (BNWF) models with prescribed soil reaction *p-y* curves given by the DNV [3] and the American Petroleum Institute, or API [4]. They recommend the use of cyclic loading curves based on empirical tests performed on flexible piles under hundreds of loading cycles [5]. It is widely shown that long term cyclic loading has a considerable impact on the soil-structure interaction [6, 7, 8], including the effect of soil degradation and gap formation under cyclic loads. It is therefore important to include these mechanisms in models of OWT dynamics.

Gapping is the formation of a seperation between the foundation and soil, causing unresisted lateral motion of the foundation, and a reduction in effective soil stiffness. It is affected by the soil condition, where different soil cohesiveness will affect the subsequent cave-in of a gap under cyclic load, but it has been shown that even cohesionless soils will not cave-in completely under continuous cyclic loading [9]. Changing the properties of the soil will have an impact on the natural frequency of the OWT, which is of specific importance for soft-stiff structures in danger of resonance if they experience drift of this natural frequency. Differences have been reported between the designed natural frequency and the measured value upon operation [10], with Damgaard et al. [11] recording reduction in natural frequency likely attributed to soil erosion in the upper layers around the foundation. It is important then to include in modelling efforts how this frequency may change with soil condition over long term cyclic loading.

In this paper, a simple gapping algorithm is applied to a dynamic BNWF model of several OWT case studies, and the effect of this gapping to the natural frequency is shown for different monopile geometries and levels of loading. The results of this study will have applications in the modelling and design of OWTs, and provide estimations for the condition of the soil after reasonable loading simulations are applied.

2 THE MODEL

A BNWF concept model is used with Euler-Bernoulli beams to model the structure, and soil springs with viscous dampers to model soil reaction, as displayed in Figure 2, with M_{RNA} representing the mass of the rotor-nacelle assembly, and F the externally applied force.

Soil reaction is modelled using the hyperbolic reaction curve of Duncan & Chang [12], defined as:

$$P = \frac{k_{max} y}{1 + y\frac{k_{max}}{P_{max}}} \tag{1}$$

where k_{max} is the initial spring stiffness in N/m, P_{max} is the ultimate capacity of the spring in N, y the horizontal displacement in m and P the force in N. Masing rules [13] are used to model the unloading response upon reversal. The value of the inital stiffness k_{max} used is that of Vesic [14], which is described by:

$$k_{max} = \frac{0.65 L_{EL} E_s}{(1 - v^2)} \left(\frac{E_s {d_p}^4}{E_p I_p} \right)^{\frac{1}{12}} \tag{2}$$

where L_{EL} is the elemental length in the BNWF model, E_s the Young's modulus of the soil, ν the Poisson's ratio of the soil, d_p the diameter of the pile and I_p its second moment of area. The ultimate capacity of the pile is defined by the undrained shear strength of the soil, and given

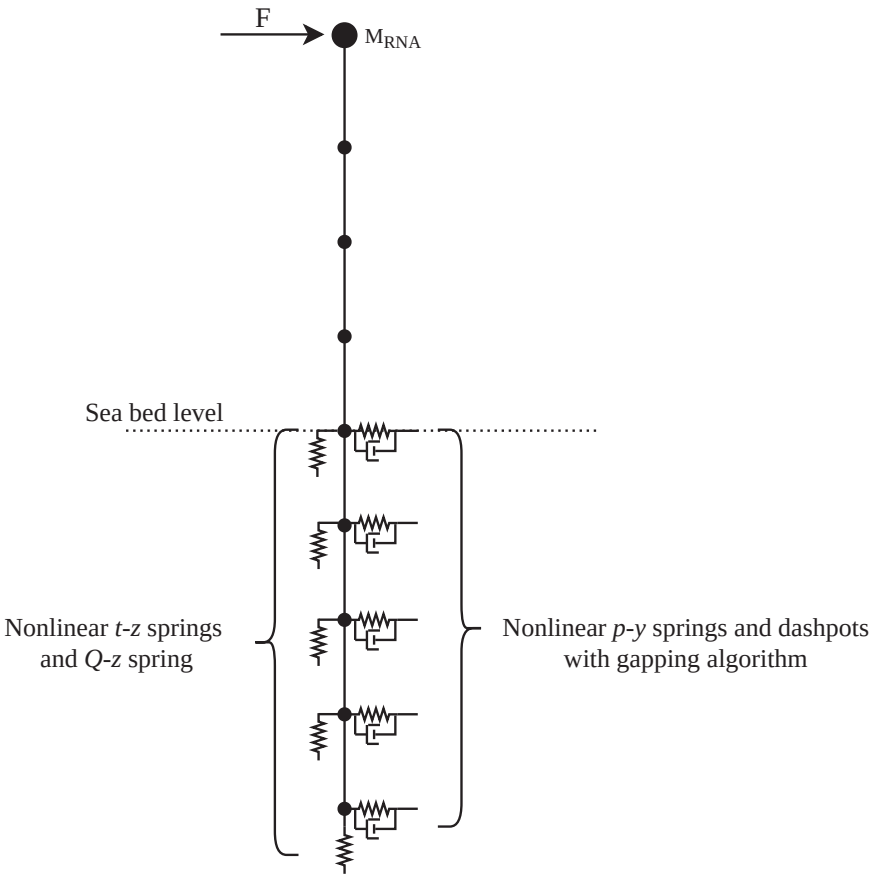

Figure 2: The BNWF model of an OWT where the lateral soil reaction is modelled with *p-y* springs and viscous dashpot dampers, and the vertical reaction with *t-z* & *Q-z* springs. The rotor-nacelle assembly is modelled as a point mass at the top node.

by [15]:

$$P_{max} = L_{EL} N_p S_u d_p \tag{3}$$

where N_p is a dimensionless coefficient increasing with depth, linearly from a value of 2 to a constant value of 11 from a depth of $z/d_p = 3$, and S_u is the undrained shear strength of the soil. Since the system is exclusively loaded laterally in this study, the axial component of the soil reaction springs can be neglected, as is commonly done for OWT analysis. A Newmark beta method [16] is used to solve the dynamic problem iteratively, with a beta value of 0.3025, and a gamma value of 0.6, in combination with a tangent stiffness method to model nonlinearity in the soil response.

2.1 Damping

Damping in the system consists of a superposition of structural, hysteretic and radiation damping. Aerodynamic and hydrodynamic damping sources are neglected for simplicity. Structural damping is modelled using the Rayleigh method, superposing contributions from the mass and stiffness matrices to form the damping matrix, and classical damping formulations for the coefficients. A damping percentage of 1% is used for structural contributions, as it is typically expected to be between 0.5% and 1.5% for OWTs [17]. Radiation damping is modelled with

the damping coefficient of Gazetas & Dobry [18], formulated as:

$$\frac{c_r}{2d_p\rho_s V_s} = \left[1 + \left(\frac{3.4}{\pi(1-v)}\right)^{5/4}\right]\left(\frac{\pi}{4}\right)^{3/4} a_0^{-1/4} \tag{4}$$

where V_s is the shear wave velocity in the soil, ρ_s is the mass density of the soil, and $a_0 = 2\pi f d_p/V_s$ is the dimensionless frequency. This damping is tuned to achieve a contribution of 0.5%.

2.2 Gapping model

The gapping model is based on an entry condition defined by the soil reaction threshold, and an exit condition based on a displacement threshold. If a node enters a gap, it experiences soil resistance only from the side shear friction, modelled with a reduced stiffness value of 5% of k_{max}. If a node is no longer in, or has not entered the gap, it continues to move based on the Masing rules and hyperbolic curve.

The entry and exit conditions are modified using parameters α_p and α_y. A node enters the gap if its p value crosses the threshold defined by:

$$p_{pos} = \alpha_p(z)\lceil p \rceil \tag{5}$$

$$p_{neg} = \alpha_p(z)\lfloor p \rfloor \tag{6}$$

for p decreasing and increasing respectively, where $\lfloor p \rfloor$ is the minimum and $\lceil p \rceil$ the maximum p value for that degree-of-freedom over the time history of loading so far. The $\alpha_p(z)$ value can be calibrated over depth z, to control the amount of gapping down the pile. Exit threshold values are based on displacement, and are defined by:

$$y_{neg}^N = \begin{cases} \alpha_y \lfloor y \rfloor & \text{if } y \leq 0 \;\&\; N = 1 \\ \alpha_y y_{neg,entry}^{N-1} & \text{if } y \leq 0 \;\&\; N > 1 \end{cases} \tag{7}$$

$$y_{pos}^N = \begin{cases} \alpha_y \lceil y \rceil & \text{if } y \geq 0 \;\&\; N = 1 \\ \alpha_y y_{pos,entry}^{N-1} & \text{if } y \geq 0 \;\&\; N > 1 \end{cases} \tag{8}$$

for p increasing and decreasing respectively, where $\lfloor y \rfloor$ is the minimum and $\lceil y \rceil$ the maximum y value for that degree-of-freedom over the time history of loading so far. The N value is the cycle number within the cyclic loading. After cycle 1, the y threshold values are derived from the displacement upon entry of the gap in the previous cycle. This means that different levels of cave-in can be modelled with the α_y parameter, with a value of 1 meaning no cave-in occurs, and a value of 0 implying a fully caved-in gap upon exit. The above parameters are shown for reference over two example loading cycles in Figure 3.

3 RESULTS

The gapping model has been applied to four case study OWTs located in the UK and Netherlands. They have been selected for their availability of geometry and soil data. The data of these OWTs is summarized in Table 1.

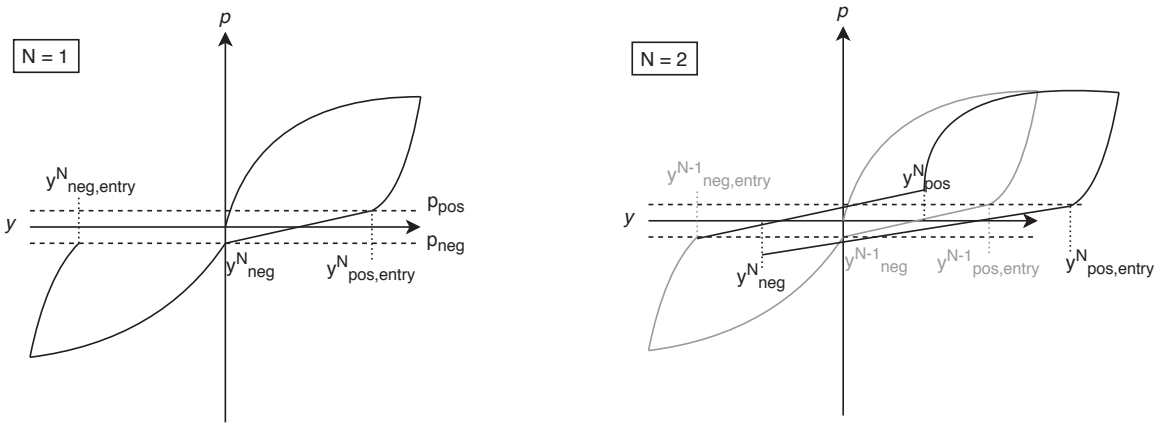

Figure 3: A schematic of a *p-y* curve for a node experiencing gapping behaviour. This figure demonstrates how the gapping parameters influence the *p-y* curve.

Parameters	Unit	Irene Vorrink	Lely A2	North Hoyle	Walney 1
Tower height	[m]	45.8	37.9	67	67.3
Substructure height	[m]	5.2	12.1	7	37.3
RNA mass	[kg]	35,700	32,000	100,000	234,500
Pile length	[m]	19	13.5	33	23.5
Pile diameter	[m]	3.5	3.2	4	6
Pile wall thickness	[mm]	28	35	30-70	80
Rotor diameter	[m]	43	40.77	80	107
Soil shear modulus G_s	[MPa]	55	53	230	70
Eigenfrequency f	[Hz]	0.563	0.634	0.35	0.35

Table 1: Parameters defining the OWT case studies. OWT geometry and soil data from [19, 20, 21].

For all case studies, the soil was modelled for simplicity as a linearly increasing stiffness value such that the average over the pile length was equal to the given value in Table 1. Environmental loading is simulated with a sinusoidal load applied to the top node and lateral degree of freedom, with an amplitude given by [19]:

$$F_{ext} = 0.5\rho_a \pi R_T^2 V_w^2 C_T(\lambda_s) \tag{9}$$

where ρ_a is the density of air, taken to be 1.25 kg/m^3, R_T is the radius of the turbine rotor blades in m, V_w the wind speed at the hub, assumed to be 13.5 m/s, and C_T is a dimensionless thrust coefficient due to the fact that the blades are rotating, dependent on the factor $\lambda_s = \frac{V_{rot} R_T}{V_w}$, where V_{rot} is the rotational speed (1P frequency) of the rotor in rad/s. The value of C_T can then be estimated from the function and graph given in [22].

The natural frequency is found by simulating a rotor-stop test, and then performing a fast Fourier transform (FFT) on the resulting period of free vibration. A rotor-stop test involves spontaneously feathering the OWT blades during operation, causing the turbine to stop spinning and the structure to freely vibrate. In this model, the OWTs are loaded with the force value given by Equation 9 sinusoidally, and then the load removed to simulate the feathering of the blades.

In this study, three rotor-stop tests are simulated; one without the gapping element, to validate

the structure geometries and soil conditions with natural frequency prediction, then two with the gapping enabled. The first is with loading equal to the value predicted in Equation 9, and a loading frequency equal to the 1P value of the OWT. The second normalises the force across all case studies, and they are loaded with a 100 kN force at 0.1 Hz to see the effect of gapping over different foundation geometries. For all tests the effect of gapping on the measured natural frequency is quantified. All the following tests were performed with representative gapping parameters of α_y = 0.5, and α_p = 0.15 at the sea bed, reducing linearly with depth with a gradient of 0.05 m^{-1}.

3.1 Validation of the gapping model

In order to validate the use of the gapping model, the results of the natural frequency analysis for an OWT in Kentish Flats are compared to the results found in the study at this wind park by Damgaard et al. [11]. The OWT, with a total superstructure length of 105.56 m, and a 29.5 m monopile was modelled with an average soil shear modulus of 60 MPa. In the experimental results used for comparison, the OWT was monitored over time with accelerometers and a number of rotor-stop tests were performed, and its natural frequency was found to vary, likely attributed to soil erosion in the upper layers of the foundation.

This OWT was modelled, and a rotor-stop test performed with gapping parameters of α_y = 0.65, and α_p = 0.25 to simulate the soil erosion. The magnitude of the force applied during the sinusoidal loading phase was selected to ensure the acceleration experienced at the top node of the OWT during free vibration aligned with the values measured during the experimental tests, for comparability. As is displayed in Figure 4, the plotted frequency spectrum found from the FFT of the free vibration, the natural frequency was predicted to vary from 0.338 Hz without gapping, to 0.327 Hz with gapping. This agrees well with the recorded data from Damgaard et al., who measured the value to vary between 0.340 Hz and approximately 0.327 Hz.

3.2 Calculated loads

Using the expression for expected external wind load in Equation 9, rotor stop tests were performed on the OWT case studies and the effect of gapping on the measured natural frequency tested. The OWTs were loaded for 20 cycles, in order to achieve steady state behaviour before the rotor-stop. Results for these tests are summarised in Table 2.

	Irene Vorrink	Lely A2	North Hoyle	Walney 1
Measured f	0.563	0.634	0.35	0.35
Modelled f (no gapping)	0.588	0.647	0.349	0.333
Modelled f (gapping)	0.572	0.596	0.329	0.129
F_{ext} [kN]	99.25	103	343	460
Slenderness ratio L_p/d_p	5.43	4.22	8.25	3.92
Change with gapping	2.72%	8.31%	5.71%	61.25%

Table 2: Eigenfrequency results for the modelled rotor-stop tests using external load calculated from Equation 9.

The results in Table 2 show first a satisfactory prediction of the measured OWT eigenfrequency assuming soil condition without gapping, using the listed OWT geometries and soil parameters. Secondly, all four results show a decrease in predicted eigenfrequency value when

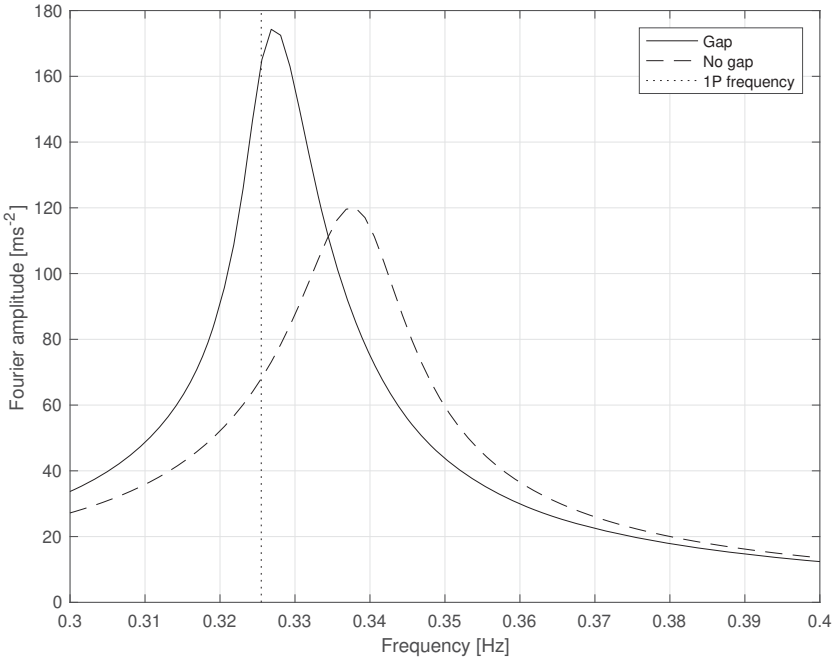

Figure 4: Frequency spectra of the Kentish Flats OWT model during the free vibration after a rotor stop test, with the gap algorithm enabled and disabled, as well as the reference 1P frequency of the OWT. The spectra resonant peaks are located at 0.338 Hz and 0.327 Hz.

the gapping is enabled. This is to be expected, since gapping essentially softens the soil response due to the transition portion of motion while in the gap which is unrestricted from soil reaction. The frequency reduction on the Walney 1 OWT is very large, due to the fact that the applied load was likely an overestimation, causing an exaggerated response.

3.3 Equal loads

The same test was then performed with the same load across all case studies, with F_{ext} = 100 kN at a loading frequency of 0.1 Hz. The resulting frequencies identified in the rotor-stop tests are given in Table 3.

	Irene Vorrink	Lely A2	North Hoyle	Walney 1
Measured f	0.563	0.634	0.35	0.35
Modelled f (no gapping)	0.588	0.647	0.356	0.338
Modelled f (gapping)	0.575	0.602	0.348	0.302
Slenderness ratio L_p/d_p	5.43	4.22	8.25	3.92
Change with gapping	2.41%	6.95%	2.25%	10.65%

Table 3: Eigenfrequency results for the modelled rotor-stop tests using a 100 kN load for all tests.

It is noted that the change in external load and loading frequency has had a small effect on the predicted frequencies without gapping, highlighting the importance of considering a variety of expected loads when predicting the natural frequency, since the value is variable over

a small range once the structure is installed. Similarly to the previous results, the inclusion of gapping has introduced a reduction in the predicted eigenfrequency, but of lower magnitude than prior due to the reduced load magnitude and frequency. However, the results suggest that the size of the reduction may be attributed to the slenderness ratio of the monopile, with the smaller (and therefore more rigid) ratios experiencing a larger change in eigenfrequency. This could be attributed to the more rigid monopiles mobilizing the soil reaction further down the monopile's length, and therefore causing a gap response over a longer pile length. The flexible monopiles can be expected to behave as fixed below a certain critical depth, and therefore will not experience any gapping below that level.

4 CONCLUSION

A simple gapping model was applied to a BNWF model of several offshore wind turbines, and the resulting effect on the natural frequency quantified. The natural frequency was identified with simulations of rotor-stop tests for OWTs of differing geometry and predicted external load. It was found that in all cases the natural frequency was reduced when the gapping effect was introduced, and that the effect appears more severe for the more rigid monopile foundations. The natural frequency is also slightly variable over different magnitudes of loading due to the nonlinear response of the soil, suggesting the importance of considering different weather and loading conditions for foundation design. With OWTs being designed with a natural frequency inside a narrow corridor of stability, it is important then to reliably predict by how much it is likely to drift throughout the operational lifetime. Including soil erosion effects like gapping may, then, assist in the design process and allow for reliable predictions. As well as application to the regular two-way dynamic loading used in this study, the model can be further included for use in stochastic loading simulations, such as more realistic wind and wave loads, and certainly has potential application to the impact of seismic loading on monopile foundations.

5 ACKNOWLEDGEMENTS

The authors gratefully acknowledge the University Research Studentship Award which has supported the work presented in this paper.

References

[1] S. Bhattacharya. Challenges in Design of Foundations for Offshore Wind Turbines. *Engineering & Technology Reference* (2014).

[2] D. Lombardi, S. Bhattacharya, and D. Muir Wood. Dynamic soil-structure interaction of monopile supported wind turbines in cohesive soil. *Soil Dynamics and Earthquake Engineering* (2013).

[3] DNV/Risø. *Guidelines for Design of Wind Turbines - 2nd Edition*. 2002.

[4] API. API RP 2A - Recommended Practice for Planning , Designing and Constructing Fixed Offshore Platforms — Working Stress Design. *Api Recommended Practice* (2007).

[5] M. Achmus, Y. S. Kuo, and K. Abdel-Rahman. Behavior of monopile foundations under cyclic lateral load. *Computers and Geotechnics* 36.5 (2009), pp. 725–735.

[6] M. Arshad and B.C. O'Kelly. Analysis and Design of Monopile Foundations for Offshore Wind-Turbine Structures. *Marine Georesources and Geotechnology* 34.6 (2016), pp. 503–525.

[7] L. Cui and S. Bhattacharya. Soil–monopile interactions for offshore wind turbines. *Proceedings of the Institution of Civil Engineers: Engineering and Computational Mechanics* 169.4 (2016), pp. 171–182.

[8] G. Nikitas, Nathan J. Vimalan, and S. Bhattacharya. An innovative cyclic loading device to study long term performance of offshore wind turbines. *Soil Dynamics and Earthquake Engineering* 82 (2016), pp. 154–160.

[9] R.T. Klinkvort. *Centrifuge modelling of drained lateral pile - soil response: Application for offshore wind turbine support structures*. PhD thesis. Technical University of Denmark, 2012.

[10] L. Arany, S. Bhattacharya, S. Adhikari, S.J. Hogan, and J.H.G. Macdonald. An analytical model to predict the natural frequency of offshore wind turbines on three-spring flexible foundations using two different beam models. *Soil Dynamics and Earthquake Engineering* 74 (2015), pp. 40–45.

[11] M. Damgaard, L.B. Ibsen, L.V. Andersen, and J. K.F. Andersen. Cross-wind modal properties of offshore wind turbines identified by full scale testing. *Journal of Wind Engineering and Industrial Aerodynamics* 116 (2013), pp. 94–108.

[12] J.M. Duncan and C. Chang. Nonlinear analysis of stress and strain in soils. *Journal of Soil Mechanics & Foundations Div* (1970).

[13] G. Masing. Eigenspannumyen und verfeshungung beim messing. *Proc. Inter. Congress for Applied Mechanics*. 1926, pp. 332–335.

[14] A.B. Vesic. Bending of beams resting on isotropic elastic solid. *Journal of Engineering Mechanics Division* 87 (1961).

[15] H. Matlock. Correlation for design of laterally loaded piles in soft clay. *Offshore technology conference*. Offshore Technology Conference. 1970.

[16] N. M. Newmark. A method of computation for structural dynamics. *Journal of the engineering mechanics division* 85.3 (1959), pp. 67–94.

[17] R. Shirzadeh, C. Devriendt, M. A. Bidakhvidi, and P. Guillaume. Experimental and computational damping estimation of an offshore wind turbine on a monopile foundation. *Journal of Wind Engineering and Industrial Aerodynamics* 120 (2013), pp. 96–106.

[18] G. Gazetas and R. Dobry. Simple radiation damping model for piles and footings. *Journal of Engineering Mechanics* 110.6 (1984), pp. 937–956.

[19] S. Bisoi and S. Haldar. Dynamic analysis of offshore wind turbine in clay considering soil-monopile-tower interaction. *Soil Dynamics and Earthquake Engineering* 63 (2014), pp. 19–35.

[20] S. Adhikari and S. Bhattacharya. Dynamic analysis of wind turbine towers on flexible foundations. *Shock and Vibration* 19.1 (2012), pp. 37–56.

[21] D. Amar Bouzid, S. Bhattacharya, and L. Otsmane. Assessment of natural frequency of installed offshore wind turbines using nonlinear finite element model considering soil-monopile interaction. *Journal of Rock Mechanics and Geotechnical Engineering* 10.2 (2018), pp. 333–346.

[22] D. Lombardi. *Dynamics of Offshore Wind Turbines*. PhD thesis. University of Bristol, 2010.